Boletín de la Sociedad Española de Cerámica y Vidrio
Vol 53, 4, 149-161, Julio-Agosto 2014 ISSN 0366-3175. eISSN 2173-0431.
http://dx.doi.org/10.3989/cyv.192014

BOLETIN DE LA SOCIEDAD ESPAÑOLA DE
Cerámica y Vidrio
ARTICULO DE REVISIÓN

EPD-deposited ZnO thin films: a review

M. VERDE

Instituto de Cerámica y Vidrio (CSIC).
Kelsen 5, 28049 Madrid (España)

ZnO-based materials and specifically ZnO films with tailored morphology have been subjected to extensive research in the past few years due to their high potential for multiple prospective applications, mainly in electronics. Electrophoretic Deposition (EPD) constitutes an economical, ecofriendly, low energy consuming and easily scalable alternative to the high energy consuming evaporative techniques which are commonly used for the obtaining of these ZnO films. For its application, however, the use of stable, well dispersed suspensions is a necessary requirement, and thus a thorough study of their colloidal chemistry is essential. In this work the main contributions to the study of colloidal chemistry of ZnO nanoparticle suspensions and their shaping into ZnO films by EPD are summarized.

Keywords: ZnO, Thin Films, Deposition methods, Shaping, Suspension.

Láminas delgadas de ZnO depositadas por EPD: Una revisión

Los materiales basados en ZnO y en particular las láminas de ZnO con morfología controlada han sido objeto en los últimos años de numerosas investigaciones debido al elevado potencial que presentan para múltiples aplicaciones emergentes, principalmente en electrónica. La deposición electroforética (EPD) constituye un método alternativo económico, ecológico, de bajo coste energético y elevada escalabilidad para la producción de éstas láminas de ZnO, en contraste con las técnicas evaporativas empleadas habitualmente, las cuales presentan un elevado impacto energético, así como una escalabilidad complicada. Para su aplicación, sin embargo, y puesto que el principal requisito es el uso de suspensiones estables y bien dispersas, es necesario un detallado estudio de la coloidequímica de las mismas. En este trabajo se resumen las aportaciones más relevantes relativas al estudio de los distintos parámetros que afectan a la estabilidad coloidal de las suspensiones de nanopartículas de ZnO y al proceso de obtención de las láminas mediante EPD a partir de las mismas.

Palabras clave: ZnO, láminas delgadas, métodos de deposición, conformado, suspensiones.

Cómo citar este artículo: Verde, M (2014): EPD-deposited ZnO thin films: a review, *Bol. Soc. Esp. Ceram. Vidr.*, 53 (4): 149-161. http://dx.doi.org/10.3989/cyv.192014

1. INTRODUCTION

Zinc oxide is a well-known semiconductor material which has been subject to periods of intensive research in the past, starting in first quarter of the past century and reaching its "peak" in the late 70s and beginning of the 80s [1-4]. At that moment, the requirement for materials with reduced dimensionality (in the nanoscale) and the difficulties for both p and ambipolar p-n doping it made the interest in ZnO as bulk material decrease. However, there has been a resurgence of the interest on ZnO in the past decade, fueled and fanned by the vast amount of prospects that functional ZnO nanostructures, especially ZnO thin films, present for a wide range of applications, such as chemical sensors, piezoelectric transducers and actuators, light emitting diodes, catalysts, transparent semiconductors or high speed electronic and optoelectronic devices [5-9]. This great variety of applications is mainly due to the reduction in size from bulk to thin film, which facilitates their incorporation into nanometric devices and "induces" new properties for ZnO thin films which are largely believed to be the result of surface and quantum confinement effects. In this sense, and depending on the preparation method, the properties of ZnO thin films (in advantage to the bulk material) can be tailored to show insulating or semiconducting properties, ferromagnetic behaviour, excitonic stimulated emmision, etc. In addition ZnO may replace other materials, such as wide band gap semiconductor GaN for some optoelectronic applications, or ITO as transparent semiconductor.

Such an amount of prospective applications of ZnO nanostructures is due to the unique set of physical and chemical properties of ZnO, like its direct wide band-gap (3.37 eV), its large exciton binding energy (60 meV), its strong luminescence or its amphoterism [4, 10]. Many of these properties arise from the crystalline structure of ZnO-wurtzite. Even though zinc oxide can have two other crystalline structures- zinc-blende and rocksalt-, the high polarity of the Zn-O bond accounts for the preferential formation of wurtzite rather than zinc-blende, which is metastable, or rocksalt, which can only be obtained at high pressures. In the wurtzite crystal structure, hexagonal-close-packed (hcp)

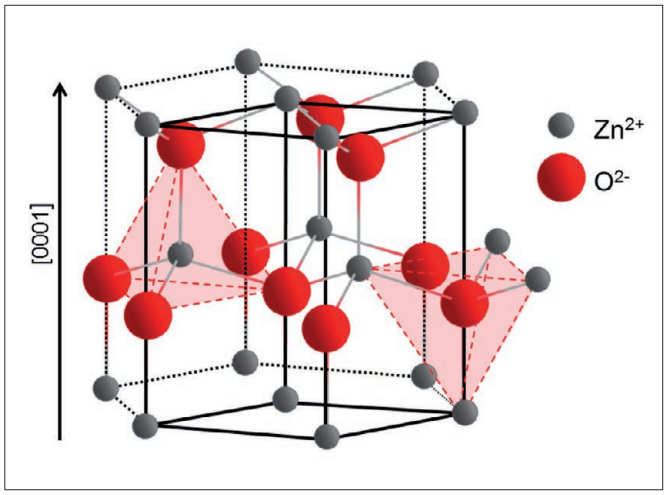

Figure 1: Representation of the crystallographice structure of wurtzite structure.

[15], RF magnetron sputtering [16], spray pyrolysis [17], metal organic chemical vapor deposition (MOCVD) [18] or pulsed laser deposition (PLD) [19]. Nevertheless, these techniques present important drawbacks, such as the high energy consumption and sophisticated instrumentation required for the transformation of the Zn precursors to the gas state, which increase their cost and make them hardly scalable. In this sense, conventional colloidal, i.e. solution-based, methods are slowly taking over interest, as they allow the economical, reliable production of ZnO films with complex shapes, small defect size/numbers, good phase dispersion and homogeneous compositions [20]. This is achieved through a careful control of the starting suspension, that has to be stable, and the different types of interparticle forces in it. Amongst these, Electrophoretic deposition (EPD) has been recognized as the most versatile technique for particulate processing due to the wide range of dimensions it can be applied to, and to its applicability to nanoparticles assembly [21].

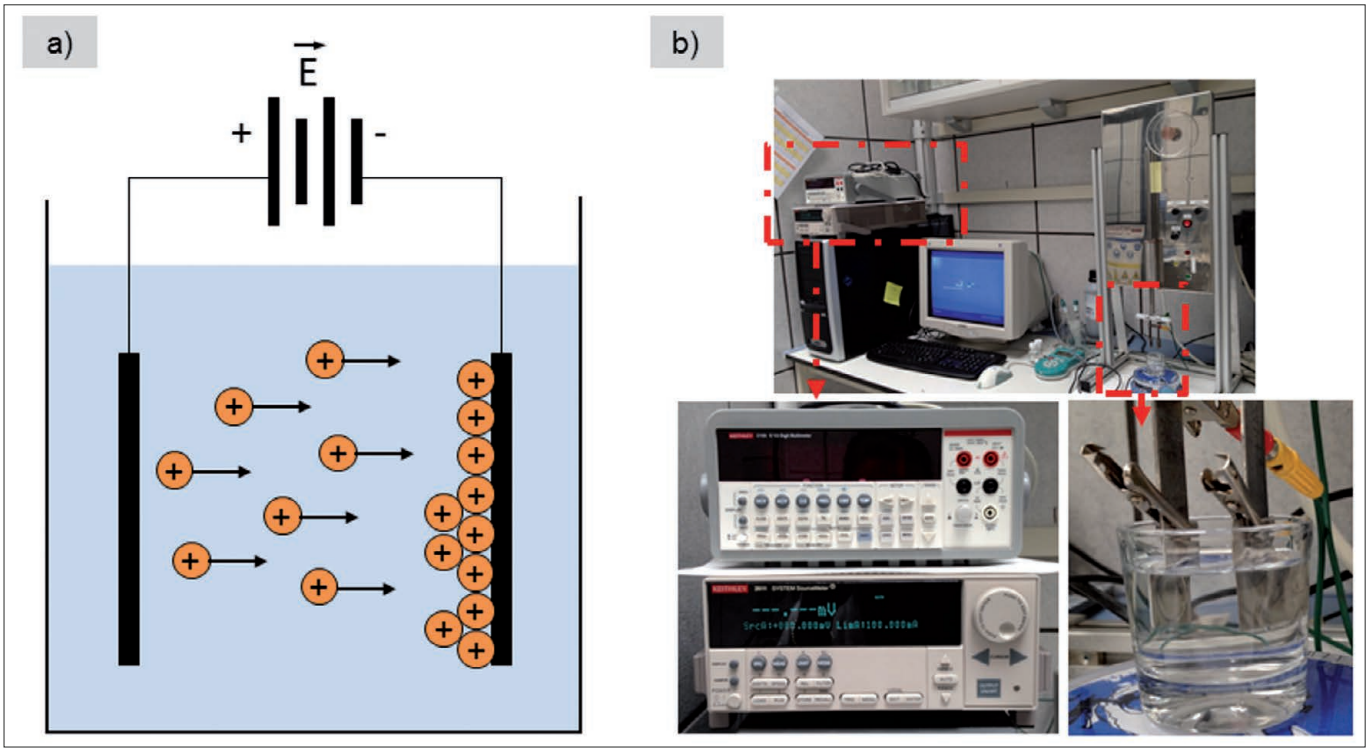

Figure 2: a) Scheme of an electrophoretic deposition cell showing positively charged particles in suspension migrating towards the negative electrode; b) Photographs of an EPD setup. The insets show the detail of the sources (left) and the cell with the immersed electrodes (right).

planes composed of tetrahedrally coordinated O^{2-} and Zn^{2+} ions interpenetrate alternatively, with the c-axis directed along the [0001] direction, giving rise to ending facets with different atoms and charges: positively charged Zn-(0001) and negatively charged O-$(000\bar{1})$ surfaces (Figure 1). This results in a normal dipole moment and a spontaneous polarization along the c-axis, as well as a divergence in surface energy. This divergence in surface energy between the different surfaces is extremely relevant to explain the reactivity of zinc oxide, its properties and its multiple growth morphologies [11-14].

The vast number of uses of ZnO films in different technological areas boosted research on ZnO thin film deposition methods, which mainly consist in non-conventional, evaporative, methods, e.g. physical vapor deposition (PVD)

The EPD process consists on the application of an electric field to a suspension containing surface-charged particles, so that these particles migrate towards an oppositely charged electrode (electrophoresis), and subsequently "accumulate" on it, forming a coherent, homogeneous deposit (Figure 2) [22]. In this sense, and in contrast to other colloidal methods, it allows the direct shaping of dense ceramic bodies from suspensions with low solid contents (< 10 g/L). Moreover, it is an easily scalable and sustainable process with minimal environmental impact (as it can be carried out in water) and renders deposits with high microstructural homogeneity and tailored thickness. The main parameters that determine the effectiveness of EPD are those related to the suspensions and their stability: suspensions must

Bol. Soc. Esp. Ceram. Vidr. Vol 53. 4, 149-161, Julio-Agosto 2014. ISSN 0366-3175. eISSN 2173-0431. http://dx.doi.org/10.3989/cyv.192014

be stable and well dispersed for particles to migrate and deposit independently.

In this context, the number of publications on Electrophoretic Deposition of ZnO, has been exponentially increasing in the past few years. These cover different topics of the EPD process, such as particles stabilization and surface charge, kinetic studies, or the use of templates, as well as the applications of the deposited ZnO thin films. The aim of this review is thus to comprehensively summarize the main advances reported in the literature for each of these topics.

2. COLLOIDAL BEHAVIOR AND STABILIZATION OF ZNO

As mentioned in the introduction, the main requirement for effective EPD is the use of stable suspensions. Therefore, understanding the surface chemistry of the material in different suspension media in order to tailor its stabilization through the different types of interparticle forces is a key parameter.

When a particle is immersed in a polar liquid medium, there is a build-up of charge at the solid liquid interface, due to different charging mechanisms [23, 24]. This surface charge influences the distribution of nearby ions in the polar medium, which rearrange in order to neutralize it, forming an electric double layer. This consists of an inner layer, known as Stern layer, formed by a monolayer of counter-ions attached to the particles surface, and a diffuse layer, in which a neutralizing excess of ions and counter ions distributed in a diffuse manner in the polar medium form an "ionic atmosphere" around the particle [25]. The resulting potential at the shear layer formed between the stern and the diffuse layer when the particle moves in the liquid is known as electrokinetic or zeta potential (ζ), and its value is proportional to the surface charge of the particle. Moreover, the pH value at which the zeta potential of a powder is zero is known as isoelectric point (IEP)[1], and its characteristic of every particle-solvent system.

The colloidal stability of a suspension is given by the total interparticle potential energy, V_{total}, which is determined by the balance between attractive Van der Waals forces (V_{vdW}), and repulsive ones, mainly double-layer (electrostatic, V_{elect}) and/or steric (V_{steric}) interactions:

$$V_{total} = V_{VdW} + V_{elect} + V_{steric}$$

In order for a suspension to be stable, thus, repulsive interactions must overcome attractive ones, ($V_t < 0$) forming an energy barrier which prevents coagulation [22]. There are three main stabilization mechanisms based on these repulsive interactions [26]:

- Electrostatic mechanism: due to double-layer repulsion between particles. Its extent is controlled by the thickness of the electrical double layers (commonly identified with the Debye length).
- Steric mechanism: based on the adsorption of polymers onto the surface of the particle, stabilization is due to the physical impediment created by the organic chains.
- Electrosteric mechanism: based on a combination of the both previous mechanisms, polyelectrolytes or charged dispersants are adsorbed onto the surface of the particles.

Experimentally, the total repulsive interaction is measured through the zeta potential of the suspensions and the determination of their IEP, which corresponds to the maximum instability of the suspension. These parameters mainly depend on the surface chemistry of the particle in the specific media, which can be tuned by modifying the surface charge of the particles.

2.1. Influence of the kind of surfaces in the colloidal chemistry of ZnO

It has been repeatedly reported in the literature how the surface chemistry of ceramic particles in suspension highly influences their dispersion and stabilization [20, 27-31]. For example, it is known that different surface chemistries of alumina powders lead to differences in pH, magnitude and sign of the dispersions mobility (zeta potential) [32] and this, in turn, leads to differences in the amount of dispersant required to stabilize the system. These different surface chemistries or charging behaviors are due to the presence of different types of surface hydroxyl groups (see Franks and Gan [33]), which arise from the "imperfect" nature of the surfaces of colloidal particles, which present edges, steps, vacancies and other defects.

Something similar occurs for ZnO. As it was described in the introduction, ZnO presents a hexagonal, non centrosymmetric structure which is polarized along the c-axis, and this gives rise to polar and non-polar facets with different reactivity. In a comprehensive review published in 2007, Woll [13] described the structure of these different facets and their distinct reactivities towards several adsorbates. In this way, he reported how for the ZnO $(010\bar{1})$ nonpolar surface with no electrostatic instabilities and truncated bulk structure, the adsorption of CO_2, CO, H_2O and H atoms gives place to ordered adlayers. However, the situation differed for polar surfaces: for the Zn-ZnO surface, the general consensus states that it essentially presents a (1x1) structure, terminated by Zn atoms and exhibits a high density of steps forming triangular terraces, which make it specially reactive to small molecules, such as H and CO and provide active sites for the dissociation of Brønsted acids [34] (see Figure 3a). Nevertheless, the most interesting surface of ZnO from a chemical point of view is the oxygen terminated polar surface, O–ZnO. In this case, there is still no convincing mechanism proposed for the removal of its electrostatic instability. There are experimental evidences that a hydrogen-terminated (1×1) O-ZnO is formed whenever ZnO is not in vaccum (though theoretically unstable) and a (1x3) reconstruction mechanism has been suggested for the clean, hydroxyl-free O-ZnO surface (although this mechanism has remained controversial). The model for this reconstruction basically consists of an ordered array of O-vacancies which renders the surface a very high reactivity (Figure 3d).

In any case, it is clear that these different surface reconstruction/stabilization mechanisms dramatically affect the surface behavior and thus the reactivity of the polar

1. The IEP shouldn't be confused with the point of zero charge (PZC), where net charge on the surface is zero. The IEP and the PZC will be the same only if there is no adsorption of other ions rather than the potential determining H+/OH- at the surface.

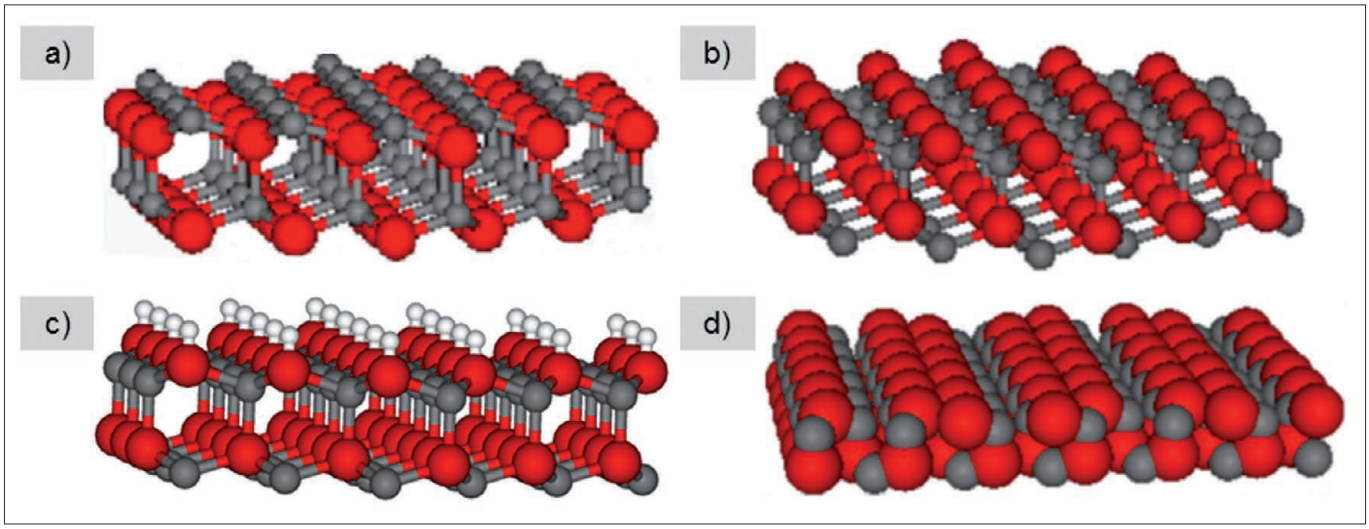

Figure 3: Structures of (a) an ideal, unreconstructed Zn–ZnO surface (b) an ideal oxygen-terminated polar surface, (c) the H-saturated (1x1) O–ZnO surface, and (d) model proposed for the (1x3)-reconstructed surface of the O–surface. Note, that all four models are electrostatically instable. Zn atoms are represented by the grey, small balls, O atoms by the red balls and H atoms by the white ones. (Adapted from [13]).

ZnO surfaces [11, 35-37], and this will have a relevant effect on the different methods used to enhance stabilization and dispersion.

2.2. Aqueous colloidal behavior of ZnO.

When metal oxides are immersed in water, formation of hydroxide layers (≡M-OH) on their surface due to hydrolysis is a very common phenomenon, as water molecules can be both physically and chemically adsorbed onto the surface of the dispersed oxide particles. It is these hydroxide layers that become charged by reacting with H^+ or OH^- species due to surface amphoteric reactions [38], giving place to positively charged surfaces at low pH values, by proton H^+ adsorptions, or negatively charged surfaces at high pH values, due to proton losses:

$$\equiv M\text{-}OH + H^+ \leftrightarrow \equiv M\text{-}OH_2^+ \qquad pH < 7 \qquad \text{(Eq.1)}$$
$$\equiv M\text{-}OH + OH^- \leftrightarrow \equiv M\text{-}O^- + H_2O \qquad pH > 7 \qquad \text{(Eq. 2)}$$

In the case of ZnO, Reichle et al. [39] established that the surface zinc hydroxide layer, ≡Zn-OH^+ or $Zn(OH)_{2(S),}$ is in equilibrium with different hydroxylated metal species in solution, whose fraction varies as a function of pH (Figure 4). In this case, the mechanisms of surface charge consist mainly on the adsorption of protons/hydroxyls onto the hydroxide amphoteric surface sites and/or the formation of hydroxylated metal species in solution which deposit on the solid surfaces, according to the following reactions [40, 41],

$$Zn^{2+}_{(aq)} + OH^-_{(aq)} \leftrightarrow Zn(OH)^+_{(aq)} \qquad \text{(Eq.1.3)}$$
$$Zn(OH)^+_{(aq)} + OH^-_{(aq)} \leftrightarrow Zn(OH)_{2\ (s)} \qquad \text{(Eq.1.4)}$$
$$Zn(OH)_{2\ (s)} \leftrightarrow Zn(OH)_{2\ (aq)} \qquad \text{(Eq.1.5)}$$
$$Zn(OH)_{2\ (aq)} + OH^-_{(aq)} \leftrightarrow [Zn(OH)_3]^-_{(aq)} \qquad \text{(Eq.1.6)}$$
$$Zn(OH)_{2\ (aq)} + 2OH^-_{(aq)} \leftrightarrow [Zn(OH)_4]^{2-}_{(aq)} \qquad \text{(Eq.1.7)}$$
$$Zn(OH)_{2\ (aq)} \leftrightarrow ZnO_{(s)} + H_2O_{(l)} \qquad \text{(Eq.1.8)}$$
$$Zn(OH)_{2\ (s)} \leftrightarrow ZnO_{(s)} + H_2O_{(l)} \qquad \text{(Eq.1.9)}$$
$$[Zn(OH)_3]^-_{(aq)} \leftrightarrow ZnO_{(s)} + H_2O_{(l)} + OH^-_{(aq)} \qquad \text{(Eq.1.10)}$$
$$[Zn(OH)_4]^{2-}_{(aq)} \leftrightarrow ZnO_{(s)} + H_2O_{(l)} + 2OH^-_{(aq)} \qquad \text{(Eq.1.11)}$$

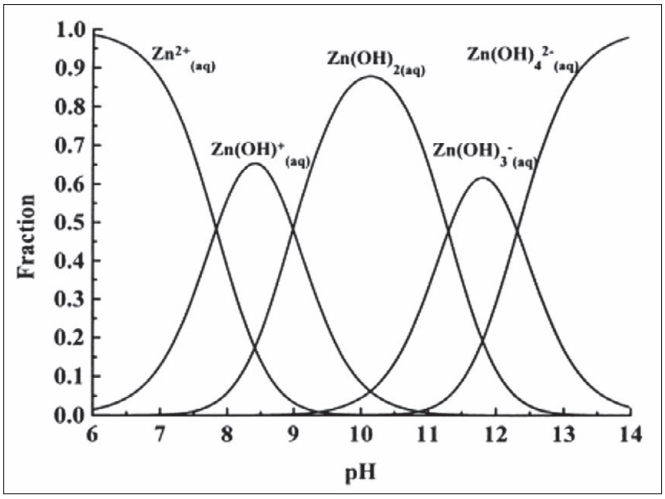

Figure 4: Fraction of Zn (II) ions species existing as $Zn^{2+}_{(aq)}$, $Zn(OH)^+_{(aq)}$, $Zn(OH)_{2\ (aq)}$, $Zn(OH)_3^-{}_{(aq)}$ and $Zn(OH)_4^{2-}{}_{(aq)}$ over a range of pH at 25 °C [39].

When, as in this case, H^+ and OH^- are the potential determining ions, the number of charge sites and the surface charge of the oxide particles are determined by the pH of the solution. Therefore, measuring the zeta potential vs. pH of a suspension will render a graphical representation of the surface charge behavior as a function of pH. According to the literature, ZnO presents its IEP at a pH ≈ 8.5 [38, 42], which implies that it will be positively charged at pH < 8.5 and negatively charged at pH > 8.5 (Figure 5a). Therefore, considering its zeta potential, ZnO can (theoretically) be stabilized by just a pH adjustment, locating the suspension at a pH far from its isoelectric point. However, the useful pH range will need to be limited to 7 < pH < 12 in order to prevent ZnO from dissolving completely (see Figure 5b).

In this sense, Degen et al. [43], following the steps of Reichle et al., carried out a thorough study of the mechanism for surface charge formation in ZnO by means of zeta potential measurements. In this work they reported that for aqueous ZnO suspensions, the surface charge development is

Bol. Soc. Esp. Ceram. Vidr. Vol 53. 4, 149-161, Julio-Agosto 2014. ISSN 0366-3175. eISSN 2173-0431. http://dx.doi.org/10.3989/cyv.192014

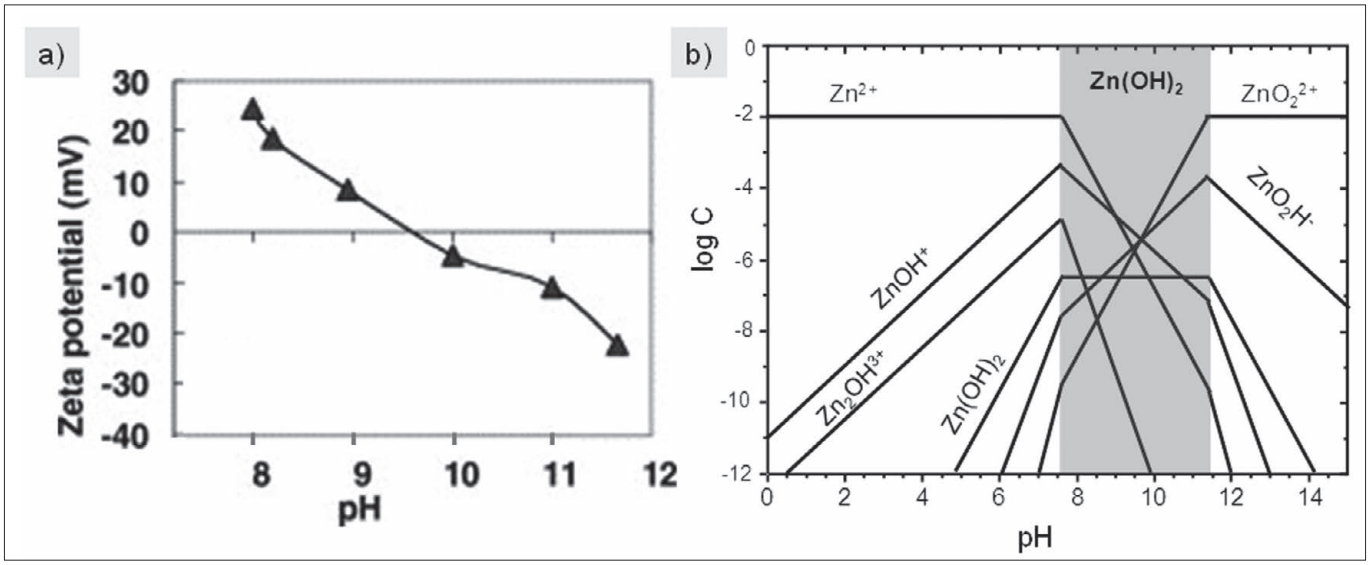

Figure 5: a) Typical zeta potential vs. pH curve of ZnO and b) log [Zn^{2+}] vs. pH diagram. The area lighted in blue corresponds to the predominance pH range of $Zn(OH)_2$.

governed by the adsorption of different zinc hydroxo species, in agreement with the results of Reichle et al. Moreover, they studied the stabilization of these suspensions through pH adjustment and zeta potential measurements, and in this way they established that pure electrostatic stabilization of was not possible in the range 7.2 < pH < 12, in which the isoelectric point of ZnO is included (Figure 5).

Thus, it can be concluded from these results that, in practice, the effective design of stable aqueous ZnO suspensions based only on electrostatic stabilization is not trivial, and the use of external surface charge modifiers is a key parameter, as will be discussed in the following section.

2.3. Use of surface charge modifiers

There are four main mechanisms through which a particle can acquire surface charge: (a) Preferential adsorption of ions, (b) Differential Solution of Surface Ions, (c) Isomorphic Substitution of ions, or (d) Physical adsorption of charged species onto the surface [44]. Mechanisms (a) and (b) have already been described somehow previously (see previous section) and mechanism (c) is most common for clay materials, hence this work will basically focus on mechanism (d), which refers to steric or electrosteric stabilization, i.e. the use of dispersants.

Dispersants are generally organic molecules (often polymeric in nature) adsorbed onto the particles surface to induce repulsion. In order to be effective, dispersants need to fulfill some requirements: the adsorbed layers must be of sufficient thickness to overcome van der Waals attraction, dense enough to avoid bridging flocculation between particles and anchored firmly enough to avoid desorption during particle collisions. Moreover, these dispersants/polymers can present ionizable groups (such as carboxylic or amine groups), case in which they are known as polyelectrolites, and the stabilization mechanism is considered to be electrosteric.

Surprisingly, despite the results reported by Degen et al., only few works have focused on the stabilization of ZnO suspensions through steric or electrosteric mechanisms. Amongst these, Tang et al. [45] studied the stabilization of ZnO nanoparticles through steric stabilization, by surface modification with polymethacrylic acid (PMAA). The authors reported the interaction between the surface hydroxide layer in ZnO with the carboxylic groups of PMAA, resulting in the formation of poly(zinc methacrylate) complexes on the surface of the nanoparticles. In this way, the polymer became grafted onto the particles, and its organic chain provided a steric hindrance which prevented their aggregation. Similarly, Liufu et al. [46] investigated the adsorption of polyethylene glycol (PEG) onto the surface of ZnO nanoparticles. In this case they observed that adsorption took place through hydrogen bonds with the zinc hydroxilated species on the surface of the nanoparticles, and thus was affected by pH changes. In addition, they noticed an increase in the amount of adsorbed polymer with increasing molecular weight, which was ascribed to the greater participation of loop and tail segments at the oxide/polymer interface, that favor a thicker adsorption layer. The adsorption of PEG led to a small shift of the isoelectric point of ZnO towards lower pH values, which was also more pronounced with increasing molecular weight. This shift was attributed to both the displacement of the slippage plane away from the surface, and the blocking of active sites on the surface of ZnO nanoparticles by the adsorbed polymer.

On the other hand, Tang, Uchikosi and Sakka analyzed in several publications the use of charged polymers, i.e., polyelectrolyes, as surfactants to disperse zinc oxide nanopowder (nano-ZnO) suspensions by modifying their surface charge [47, 48], i.e. by electrostatic stabilization. These authors reported how the use of a cationic polyelectrolyte, Polyethylenimine (PEI) allowed the effective stabilization of ZnO nanopowders in water, as the amino groups in it readily adsorbed protons in solution, thus providing the ZnO surfaces with a high positive charge over a large pH range. In this way PEI shifted the isoelectric point of ZnO from pH= 9.5 to pH > 11, increasing the working range in which EPD could be carried out (see Figure 6a). In a second publication, the same authors reported the stabilization of ZnO with an anionic polyelectrolyte, Polyacrylic Acid (PAA) [48]. In this case the polyelectrolyte provided a negative surface charge and no IEP was observed (see Figure 6b). In both cases, using PEI and PAA, stable ZnO suspensions were obtained from which uniform and bubble-free nano-ZnO films were deposited.

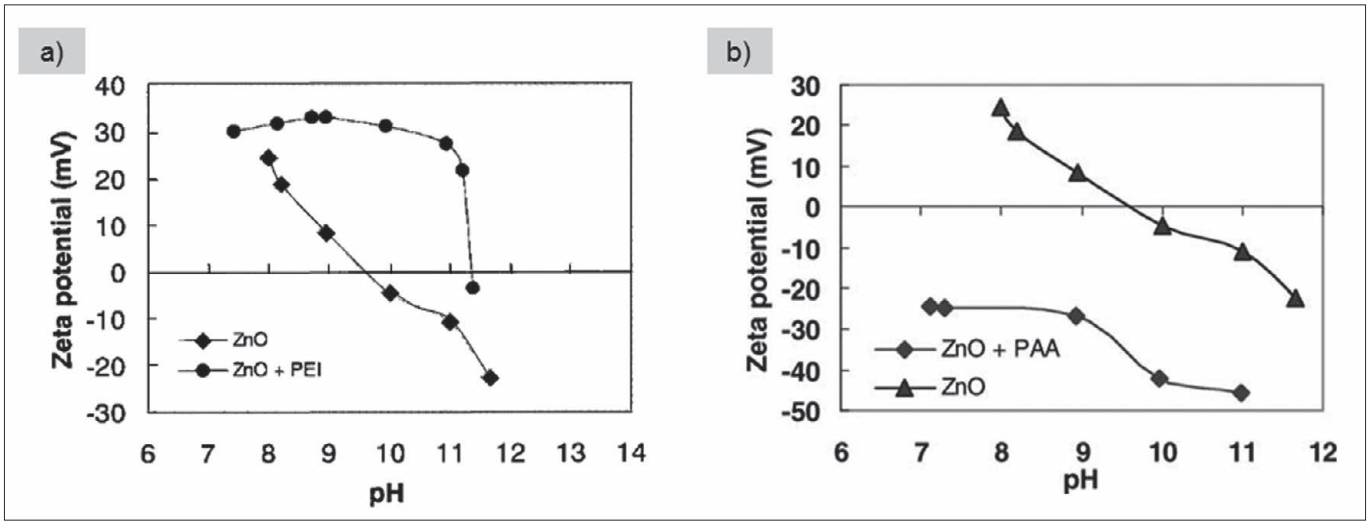

Figure 6: Zeta potential vs pH curves of ZnO suspensions with a) polyethylenimine and b) ammonium polyacrylate as dispersants (adapted from [47, 48]).

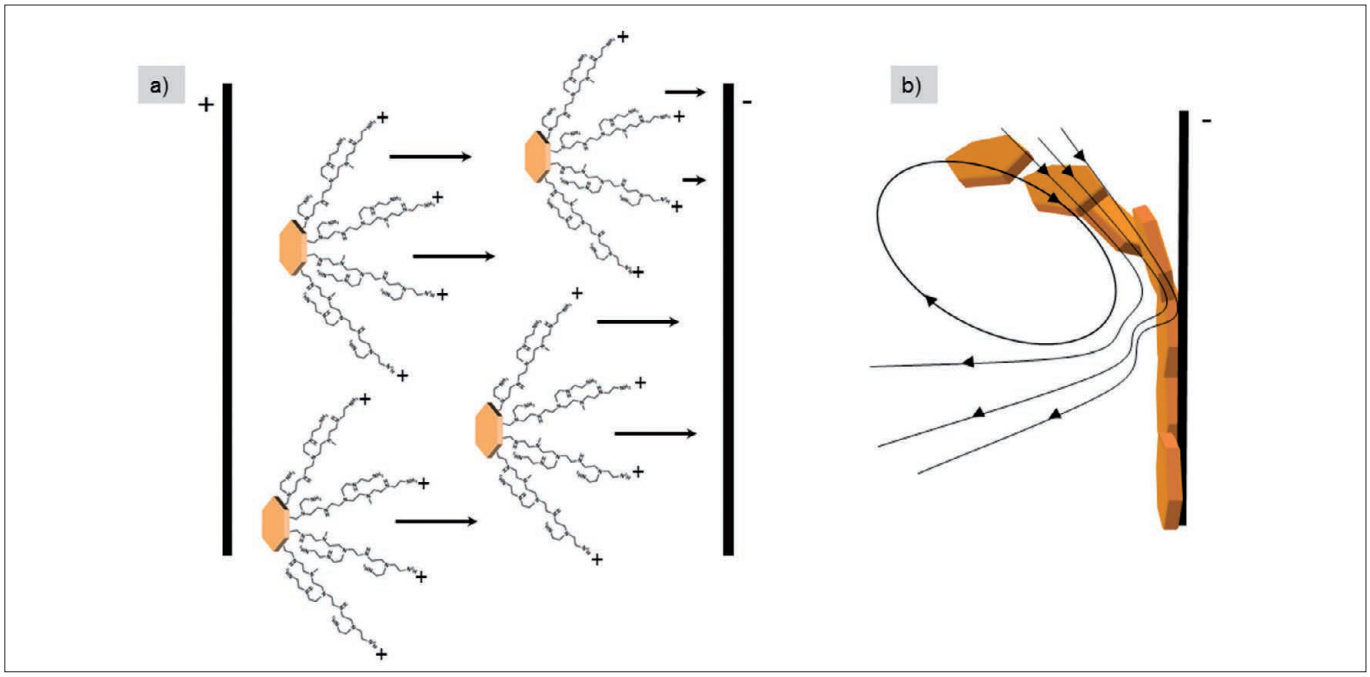

Figure 7: Scheme of a) the suggested movement of the ZnO nanoflakes with the attached PEI during electrophoresis and b) orientation of the flakes according to hydrodynamics in the area close to the electrodes surface (from [50]).

Based on the work of Tang et al., Verde et al. optimized the amount of PEI necessary for stabilization of ZnO nanoflakes [49] and studied the influence of the amount of dispersant (in weight %) on the dispersion of the powders through particle size measurements. In a subsequent article, these same authors analyzed the influence of the molecular weight of PEI on its dispersion effect by means of zeta potential vs pH measurements, observing that the polyethylenimine with the highest molecular weight (Mw=25000) provided a larger electrostatic stabilization than those with smaller chains at the same adsorption pH (between 7 and 8) [50]. This was ascribed to its large size: even though the number of charges per monomer of organic chain is always the same, regardless of the molecular weight, and despite the fact that a smaller number of chains of the PEI with the highest molecular weight were able to anchor to the surface of the ZnO nanoflakes, these were much larger than those of the other two PEIs, and therefore, provided much more charge, as they had a higher number of charged PEI monomers. This implies that even though all PEIs were adsorbed at the same pH, the PEI with higher molecular weight has a wider protonation range [51]. Moreover, these authors suggested that a preferential adsorption of PEI onto negatively charged O-ZnO surfaces takes place, giving rise to a "jellyfish-like" structure, which along with hydrodynamic forces, would direct the preferential orientation of the ZnO nanoflakes upon deposition (Figure 7).

Similarly, Dange et al. measured the adsorption of three anionic additives - polyacrylic acid (PAA), polystyrene sulfonate (PSS), and hydroxyethylidene diphosphonic acid (HEDP), onto ZnO nanoparticles in order to evaluate their dispersion efficiency [52]. They observed that the adsorption process was different depending on the amount of dispersant added: at low additive concentrations, the additives formed complexes with Zn^{2+} ions in solution which became totally adsorbed onto the particles, whereas

Bol. Soc. Esp. Ceram. Vidr. Vol 53. 4, 149-161, Julio-Agosto 2014. ISSN 0366-3175. eISSN 2173-0431. http://dx.doi.org/10.3989/cyv.192014

TABLE 1. SUMMARY OF THE POLYELECTROLYTES USED FOR THE STABILIZATION OF AQUEOUS ZNO SUSPENSIONS FOR EPD.

Name	Kind of Polyelectrolyte	Monomer structure	Ionization pH range	Ref.
Polymethacrylic acid (PMAA)	Anionic	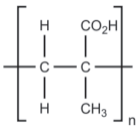	2.5-12	[45]
Polyethylene glycol (PEG)	Anionic	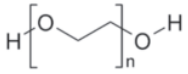	-	[45]
Polyethylenimine (PEI)	Cationic	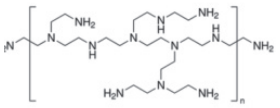	2-10 (low Mw)/ 2-12 (high Mw)	[45]
Polyacrylic Acid (PAA)	Anionic	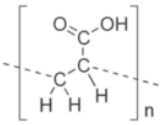	3.5-12	[48] [52]
Polystyrene sulfonate (PSS)	Anionic	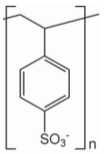	-	[52]
Hydroxyethylidene diphosphonic acid (HEDP)	Anionic	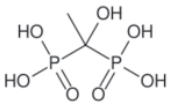	1.3-11	[52]

at high concentrations, the excess additive remained in the solution inducing a significant release of Zn^{2+} ions ions from the particles (ZnO dissolution) to form soluble zinc–organic complexes.

A summary of the reported surface charge modifiers used for the stabilization of ZnO suspensions for EPD is shown in Table 1.

2.4. Non-aqueous ZnO suspensions

Even though the synthesis of colloidal ZnO nanoparticles in non-aqueous, mainly alcoholic media has been known since the 1980`s (see article by Bahnemann et al. [53]), stabilization of these suspensions has been scarcely studied in depth, and visual inspection was the main method used for the determination of their stability.

The first report in this sense was that by Logtenberg and Stein, in which they studied the influence of water content and the effect of acid or alkali hydroxides in the zeta potential and coagulation of several alcoholic ZnO suspensions (in methanol, ethanol and propanol) [54]. In this report they described how the addition of water gave place to a shift of zeta potential to more positive values in ethanol and propanol, due to a shift of the acid/base balance of the particle/solvent system. Moreover they described that the addition of high concentrations of acid or alkali the conventional trends in zeta potential (more positive values at low pH and more negative values at higher pH) are reversed, due to the stimulated adsorption of the counter ions.

More recently, Gashghaie et al. reported the stabilization of commercial ZnO nanopowders in acetone and isopropanol, and the influence of the media on the deposition [55]. The most stable suspensions were obtained after washing the as-received powder and suspending it in acetone. However, films deposited from this media showed a low density and a high number of cracks, due to its fast evaporation rate, which leaded to intense shrinkage.

A wide number of authors have studied the surface reactivity of ZnO colloids synthesized following the method reported by Bahnemann et al. [56-60]. Most of these works came to the conclusion that surface defects of the ZnO nanoparticles were passivated by acetate ions from the synthesis procedure, and that it is the presence of these acetate groups what enhances the stability of the ZnO nanoparticles in the alcoholic media, acting as spacers and quenching the attractive van der Waals forces. In this context, Wang et al. [61] reported that the addition of base produces an increase in zeta potential with pH, due to an increase in the number of acetate groups, and thus in the number of protons and polar molecules that react with the double layer of ZnO particles in the suspension. On the other hand, Sun et al. [62] reported the stabilization of ZnO methanolic suspensions by addition of hexane, observing that suspensions with higher amounts of hexane remained stable for longer times. However, they could not determine the exact mechanism responsible for this stabilization, and instead suggested that it might be due either to the reduction of the polarity of the solvent around the ZnO nanoparticles, or due to the lowering or the free energy of the nanoparticles upon hexane addition.

Finally, a small number of publications can be found describing the use of dispersants for the stabilization of alcoholic ZnO suspensions. For example, Ma et al. [63] described the treatment of ZnO nanoparticles with 3-methacryloxypropyl trimethoxysilane, i.e. KH570, a coupling agent, which formed covalent bonds with the hydroxyl groups on the surface of the ZnO nanoparticles and changed their nature, from hydrophilic to hydrophobic, thus improving their dispersion. Hong et al. [64] used the same coupling agent, followed by radical grafting polymerization of styrene chains, which reduced the aggregation of nanoparticles and gave place to stable suspensions in organic solvents. A different example was reported by Wu and Zhitomirsky [65], in which they used dopamine (DA) and alizarin yellow (AY) as charging additives and dispersants for cathodic and anodic EPD (respectively) of ZnO suspensions in ethanolic media.

3. KINETICS OF EPD OF ZNO

Kinetics of EPD is a topic which has been widely discussed in the literature, as summarized in the comprehensive review by Ferrari et al. [138] and some aspects of which, such as the reactivity of the electrode/electrolyte interface, are still controversial. In this sense, the most accepted model is that by Sarkar and Nicholson [22],

$$m(t) = m0(1 - e^{-t/\tau})$$

which relates the deposited mass, m (g), and deposition time, t (s), with a characteristic time scale (τ), which in turn considers the effect of the variation of particle concentration with time:

$$\tau = V/f\mu SE$$

where V is the volume of suspension, which remains unchanged with time, μ the electrophoretic mobility, ($cm^2 \cdot V^{-1} \cdot s^{-1}$), E the electric field ($V \cdot cm^{-1}$) and S the deposition area (cm^2). Moreover, this model introduced an an efficiency factor or "sticking parameter", $f \leq 1$ (i.e. if all the particles reaching the electrode take part in the formation

of the deposit $f = 1$) so as to quantify the effect of the undetermined process of deposition. This equation has been widely accepted and applied in the literature, as it can be reduced to the simpler Hamaker model [66] for short times and predicts deviations from linearity (occurring when EPD is carried out under constant-voltage conditions and the deposit resistivity is higher than that of the suspension).

Regarding EPD of ZnO powders, several authors have experimentally studied the kinetics of the process, with the aim of obtaining films with different thicknesses:

Wong et al. [67] described the electrophoretic deposition of ZnO quantum dots in their (organic) synthesis media, and determined the deposition kinetics from the change in the optical absorbance of the films, relating this with the Zn^{2+} concentration. They observed a semilogarithmic relationship of deposition mass with deposition time, stating that the EPD of quantum particles follows the rate law derived for micrometer-sized particles by Sarkar and Nicholson. This behavior has been reported by several other authors: Wang et al. [68] analyzed the critical transition time, which can be defined as the deposition time at which deposition kinetics change from a linear ($t < t_c$) to a parabolic behavior ($t > t_c$), i.e. the deposition rate increases quickly at the initial stage and then approaches a steady state. They obtained ZnO films with varying thicknesses by varying the applied voltage and deposition times. Taking into account these results, the authors stated that kinetics of the deposition process are directly determined by the deposit layer thickness, and considered the voltage drop and suspension concentrations to be responsible for the deposition kinetics deviation from linear growth. Something similar was observed by Lommens et al. [69] when depositing thin layers of ZnO quantum dots. They analyzed the influence of the applied voltage, deposition time and quantum dot concentration on the final layer thickness, and obtained ZnO layers with thicknesses ranging from a few QD monolayers to 250 nm by applying voltages ranging from 20 to 60 V. However they reported that for layers thicker than a few monolayers, the deposition rate was considerably smaller than the theoretically calculated value, which points towards a strong screening of the electric field by the deposited ZnO layer. This observation was confirmed by Balaji et al. [70], who reported a sharp decrease of the current density for deposition times higher than 50 seconds. In addition, Miao et al. [71] studied the influence of other parameters, such as aging treatment of ZnO nanocrystallites and suspension concentration on the deposit weight. When the applied voltage and deposition time were kept constant, the deposit weight increased almost linearly with an increase in suspension concentration, but decreased for aging times above 3 days-due to agglomeration.

From these results it can be concluded that even though the kinetics of EPD for ZnO suspensions follow the model by Sarkar and Nicholson, growth of the films thickness seems to stop after a short time, probably due to a blocking of the electric field by the deposited ZnO films. However, further studies are necessary in order to verify this assumption.

4. USE OF TEMPLATES

The obtaining of deposits with specific shapes is tackled in the bibliography on EPD of ZnO through the use of templates. Some of the most widely used templates are anodic alumina membranes (AAM): Wang et al. reported in several publications [61, 72-75] the deposition of uniform and aligned ZnO nanowire arrays embedded in AAMs. In these publications they observed that the morphologies of ZnO nanowire arrays and current-time curves during EPD were determined by the breakdown behaviors of AAM templates and the applied voltages. In this sense, two different morphologies due to the voltage dependent filling characteristics of AAM were obtained: fibrils, tubules, and the mixed product (see Figure 7) [74, 75]. Moreover, it was reported how, under a given electric field, the influence/effect of zeta-potential on determining the deposition rate of ZnO nanowire arrays was higher than that of the particle size. On the other hand, and as opposed to the results reported by Miao et al. for films, these authors observed that with an increase in the colloidal concentration the growth rate of ZnO arrays embedded in AAM was decreased, while the crystallite size was enhanced [72]. This was ascribed to the higher viscosity of concentrated suspensions, which inhibited particle transportation in the solution, and to the fact that the equilibrium speed of the particles would increase with decreasing coloidal concentration. In addition, they analyzed the annealing effects on microstructure and dielectric breakdown of amorphous AAM templates [73].

Despite the fact that AAM are the most common ones, some authors reported the use of different templates. A good

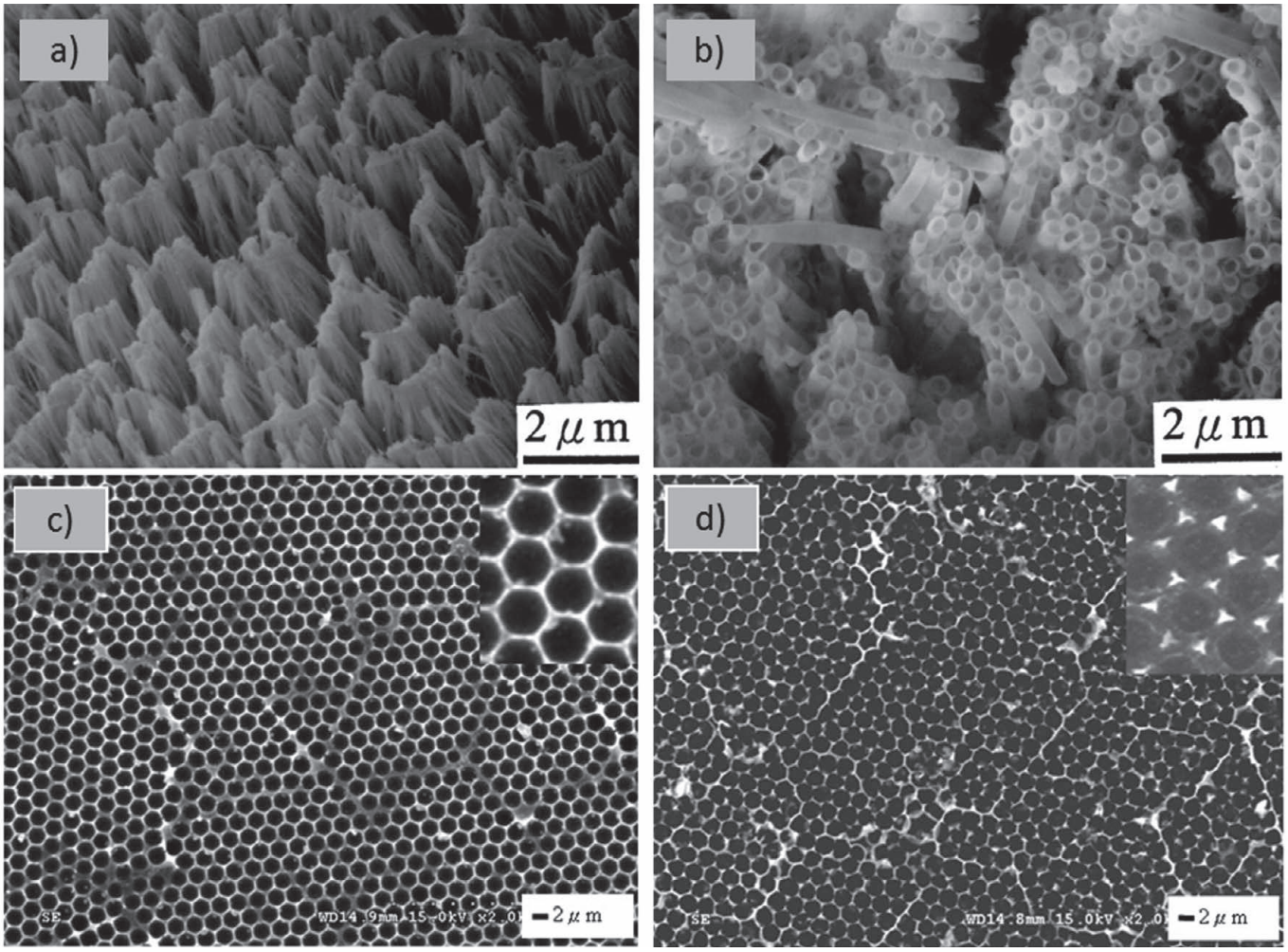

Figure 8: SEM micrographs of the different reported morphologies obtained using templates during EPD: a) and b) nanofibrils and nanotubules obtained using AAM templates under low and high voltages, respectively (adapted from [74]); c) hollow hexagonal-patterned network structures and d) hexagonal-patterned hollow ZnO triangular dots obtained using a polystyrene monolayer template (adapted from [78]).

example are the works by Chung et al. [76, 77] which reported the use of colloidal crystal templates, whose nanochannels become filled during EPD in order to obtain high quality ZnO inverse opal. In this case an accurate control of the kinetics in the interstitial spaces of the colloidal template becomes a key issue, in order to fill the colloidal template completely, avoiding jamming of the nano-channel. On the other hand, Lee et al. [78] described the fabrication of 2D ordered arrays of ZnO hierarchical structures with micro and nanopores by combining polystyrene nanosphere lithography (NSL) and EPD processes. Moreover, they successfully tailored the effect of charge balance between the colloidal particles and the polystyrene sphere-coated template to prepare arrays of ordered solid or hollow dots/network structures, determining that the mechanism governing the filling characteristics is ruled by the surface charge of the nanoparticles and the template: when the ZnO nanoparticles have the same surface charge as the template ordered solid dots are obtained, whereas if they have opposite charges hollow structures are produced.

An opposite approach to those reported in this section was reported in the most recent article by Verde et al., in which thin films of two different ZnO powders were deposited by EPD in order to act as templates for the subsequent hydrothermal growth of ZnO nanostructures [79]. In this case they observed that the nature of the ZnO template deposited by EPD greatly influenced the morphology of the ZnO structures after the growth.

Figure 8 shows a summary of the different morphologies of ZnO films obtained by EPD described in this section.

5. APPLICATIONS OF ZNO FILMS OBTAINED BY EPD

Most of current literature on electrophoretic deposition of ZnO tends to focus on the properties and applications of the deposited ZnO films on different areas, rather than on the EPD process itself. Even though there is a small number of publications on miscellaneous applications of ZnO films prepared by EPD, such as catalysts, as reported by Haas-Santo et al. [80], and Nedyalkova et al. [81] or as superhydrophobic coatings on aluminum alloy surfaces to prevent corrosion, as recently reported by Huang et al. [82], most of the publications can be grouped into three main applications: gas sensors, photoluminiscent materials and dye sensitized solar cells. The literature on these applications, from "traditional" to more innovative ones, will now be briefly discussed.

5.1. Gas sensors

ZnO nanostructures have been widely used for sensing applications, due to their high sensitivity to their chemical

environment. The sensing mechanism is based on variations in the electrical resistivity of the ZnO nanostructures upon adsorption of gas molecules, which interact with the different species on the ZnO surface (see section 2.1). However the use of EPD for the preparation of ZnO films for gas sensing presents some difficulties. These lay mainly in the nature of the substrate: electric conductive substrates are necessary for EPD, however these would lower/cancel the response of the gas sensing film, as the resistance of the conductive substrate would be comparable with that of the film [83, 84]. Thus, the used substrate should be conductive in EPD and insulating in gas sensing.

In this sense, the first report on the fabrication of a resistive ZnO gas sensor prepared by EPD was published by Hossein-Babaei et al.[85]. In it they used AI-Cr-Fe alloy substrates, which were fired at 1000 °C after EPD, forming a native aluminium oxide insulating layer between the ZnO later and the metallic substrate. The ZnO films obtained in this way acted as linear smoke detectors, showing a 2 % conductance change per ppm of wood smoke contamination and a fast resistance recovery. Some years later, Dougami et al [86] reported that modification of SnO_2-based bead gas sensors by ZnO coatings prepared by EPD greatly enhanced their sensitivity to H_2 and C_2H_5OH. Moreover, this ZnO coating also acted as a catalyst layer. Along these lines Rout et al. [87, 88] carried out a comparative study of the hydrogen and ethanol sensing characteristics of different types of ZnO nanostructures (nanorods and nanowires) deposited by EPD which revealed that nanorods and nanowires prepared in alumina membranes are outstanding sensors at or below 150 ºC. In addition, these sensitivities were not significantly affected by humidities up to 50 % and could stand up to 1000 cycles.

The latest work on the topic was published in 2010 by Han et al.[89], describing the use of Anodic aluminum oxide (AAO)/Al composite structures as substrates for the deposition of Ga-doped ZnO (GZO) dispersed in different media. It was observed that this kind of substrates could be successfully used as substrates for EPD, due to their relatively thinner barrier layer. The thickness of the AAO was proportional to the current density and preparation time, and thus the different resistance was gained: thin AAO was appropriate for gas sensing films with lower resistance, while thicker AAO was more adequate for gas sensing films with either lower or higher resistances. Moreover, it was reported that the EPD had to be carried out in alcoholic media (ethanol), as the production of H_2 in the cathode during aqueous EPD destroyed the AAO substrates. The films prepared in this way showed a gas response of 0.05–0.1 to 1ppm formaldehyde.

5.2. Photoluminiscent materials

Another classical application of ZnO films is as photoluminiscent materials, as they have been repeatedly reported to have strong UV emission [90-93]. In this context, Jeon et al. reported the use of electrophoretic deposition of ZnO:Zn phosphors for their application as anode plates in field emission displays [94], which require densely packed thin screens of nanoparticles to be produce in a reproducible way. The authors studied the influence of $Mg(NO_3)_2$ concentration (used to obtain MgO, which acts as binder), deposition time, and applied electric field in order to optimize the deposited amount of phosphors for a maximum brightness and cathodoluminescence. It was observed that the deposited amount of phosphor was inversely proportional to the salt concentration, which increased the interparticle repulsion and decreased their mobility. However, this could only be lowered up to a certain point, as concentrations of $Mg(NO_3)_2$ lower than 10^{-5} M rendered films with very low adhesion. In this sense, the best luminescence results, 360 cd/m^2, were obtained for films with concentrations of $5{\cdot}10^{-4}$ M, screen weights of 2.9 mg/cm^2, and thickness of 9.8 μm.

More recently, Ma et al. [95] reported the improved field emission properties of ZnO films with tetrapod morphologies. These ZnO tetrapod films showed emission current densities as high as 1.96 mA/cm^2 with thicknesses of 150 μm (higher than those obtained for ZnO films deposited by other techniques) and excellent field emission stability, which make them promising candidates for future applications as high brightness electron sources.

On a related topic, Wang et al. reported the photoluminiscent efficiency of high quality films obtained from EPD of amorphous ZnO nanopowders [96]. These films displayed quasi-three-dimensional quantum confinement effects which greatly affected the photoluminiscent efficiency, showing a dramatic increase in the UV emission intensity. These results were ascribed to the amorphous nature of the ZnO powders in the film. Interestingly, Zhang et al. [97] reported very similar results for films with high quality polycristalline ZnO nanopowders. In this case, however, the authors ascribed the strong near-band-edge emission to free excitons. Along these lines, Yadav et al. [98] analyzed the UV photoconductivity relaxation of ZnO films prepared by EPD, RF diode sputtering and RF magnetron sputtering, in order to try to correlate the exact nature of photoconductivity with the crystallinity and film microstructure, so as to prepare a practical UV photodetector with enhanced response and fast speed. In this sense, and even though the EPD-as deposited films showed the largest photoresponse with fairly fast rise and decay times, the films deposited using RF magnetron sputtering represent a better option, as they presented a smaller density of defects centers (trap and recombination) than the photoexcited charge carriers concentration, and a fast and saturated photoresponse, necessary for high speed operations.

5.3. Dye Sensitized Solar Cells.

Dye-sensitized solar cells (DSSCs) are one of the most innovative applications of ZnO films prepared by EPD, as they are considered to be the new generation of photovoltaic devices, with advantages such as high energy conversion efficiencies [99-101]. ZnO photoanodes have been developed and studied as promising alternatives to the most common TiO_2 ones, due to the high electronic mobility of ZnO and to the similar band gap of both materials, ~3.2 eV for ZnO and ~3.3 eV for TiO_2. A great variety of methods have been used for the preparation of these ZnO electrodes [102-107]. However they generally involve high temperature annealing processes, which limit the kind of substrates that can be used, e.g. flexible polymer substrates can only stand temperatures up to 150 °C [108, 109]. It is at this point that EPD becomes a feasible technique for the preparation of these electrodes.

Yin et al. first reported the use of EPD for the obtaining of high performance ZnO photoelectrodes at room temperature in 2010 [110]. They described the preparation of ZnO photoanodes on FTO glass and plastic substrates, using organic dye D149 as sensitizer. The resulting DSSCs showed overall conversion

Bol. Soc. Esp. Ceram. Vidr. Vol 53. 4, 149-161, Julio-Agosto 2014. ISSN 0366-3175. eISSN 2173-0431. http://dx.doi.org/10.3989/cyv.192014

efficiencies of 4.78 % (on FTO glass) and 4.17 % (on plastic) (under 100 mW cm^{-2} AM 1.5) without any subsequent treatment. These high conversion efficiencies are ascribed to a good connectivity between the ZnO nanoparticles due to the EPD process.

In a subsequent publication, Chen et al. described the use of mechanic compression and UV–O^{3-} radiation as post-treatments after EDP, to try to enhance the connectivity between ZnO nanoparticles, and thus the light to electricity conversion efficiency of their corresponding flexible DSSCs [111]. It was observed that the efficiency of the prepared DSSCs was directly related to the applied compression, up to a critical thickness of 22 μm, over which all the photovoltaic parameters decreased. In this way, DSSCs prepared with 22 μm thick ZnO films (after compression) rendered efficiencies of 3.36 %. These efficiencies could be slightly increased by applying a UV–O3 treatment to just the ZnO film (efficiency = 3.42 %) or to the substrate first (ITO-PEN) and to the whole photoanode film second (efficiency = 4.04 %).

Hara et al. also studied the topic in several publications [112-114]. They analyzed the adsorption of different concentrations of ethanolic N719 dye solutions by measuring their adsorption isotherms, in order to determine the amount of dye that was actually adsorbed and optimize it. They found that there was an optimal concentration for the effective coverage of the films, which depended on the film structure, thickness, morphology of the material, pore size, surface area and pore volume. Moreover, it was observed that the final performance of the DSSCs heavily depended on the dye concentration, as well as on the thickness and morphology of the films. In this sense, they obtained efficiencies of 3.8 % and 2.8 % using ZnO nanorods and ZnO nanoparticles, respectively.

Yan et al. analyzed the influence of the method used for the preparation of hybrid ZnO/TiO_2 photoanodes on their performance [115]. For this purpose they prepared the hybrid photoanodes by electrophoretic deposition, screen printing, and colloidal spray coating. It was observed that the DSSCs prepared by screen printing showed the highest power conversion (1.87 %), whereas DSSC prepared by EPD showed the lowest ones (0.10 %). These low efficiency values can be ascribed to the nature of the ZnO powders, which showed a tetrapod morphology that produced non uniform structures and poor quality films. Moreover, the noticeable low values reported for the EPD-prepared films can also be due to the lack of optimization of the EPD parameters.

Finally, Sima et al. recently reported the fabrication of a DSSC photoanode made up of three ZnO stacked layers: a thin layer deposited on FTO substrate, used as blocking layer, and an array of ZnO nanorods intended to improve the mechanical stability and the adherence of the third layer, obtained by electrophoretic deposition of ZnO nanoparticles [116]. However, the DSSCs prepared in this way showed low conversion efficiencies (1.34 %) due to both a bad contact between the ZnO nanorods and the EPD-deposited film, and a to low charge transfer resistance, associated to recombination of electrons at ZnO/dye/electrolyte interface.

6. CONCLUSIONS

Electrophoretic deposition is a method which presents a great potential for the preparation of ZnO films in a simple, cost effective and reproducible way. Therefore, and even though its use is still not extended, and the total number of publications dealing with the different aspects discussed in this work does not reach two hundred, an increase in the number of publications is likely to occur in the future, given the current trend in materials processing towards more "ecologically friendly" methods, and the rediscovered interest in ZnO nanostructures. The low environmental impact of the technique (low energy consumption, can work in aqueous media), together with the good results obtained in emerging applications of the resulting ZnO films might boost the interest of researchers on it. Moreover, the field is open for discussion, as many of the topics discussed in this paper, such as the mechanisms for the stabilization of ZnO suspensions in both aqueous and organic media, as well as those directing the adsorption mechanisms of additives or the deposition kinetics are still unclear, and require of further study.

ACKNOWLEDGEMENTS

This work was carried out under the financial support from the Spanish Science and Innovation Ministry (MICINN) through the Projects MAT2009-14448-C02-01, MAT2010-16614, IPT-310000- 2010-0012 and IPT-120000-2010-33 (Spain). The author acknowledges CSIC for the concession of a Jae-Predoc 2009 fellowship, as well as Dr. B. Ferrari and Dr. A. C. Caballero for their support.

REFERENCES

1. Hirschwald, W.; Bonasewicz, P.; Ernst, L.; Grade, M.; Hofmann, D.; Krebs, S.; Littbarski, R.; Neumann, G.; Grunze, M.; Kolb, D. M.; Schulz, H. J. E., (1981): Zinc Oxide, *Curr. Topics Mat. Sci.*, 7: 143-482.
2. Hönerlage, B.; Lévy, R.; Grun, J. B.; Klingshirn, C.; Bohnert, K., (1985): The dispersion of excitons, polaritons and biexcitons in direct-gap semiconductors, *Phys. Rep.*, 124 (3): 161-253. http://dx.doi.org/10.1016/0370-1573(85)90025-0.
3. Klingshirn, C.; Haug, H., (1981): Optical properties of highly excited direct gap semiconductors, *Phys. Rep.*, 70 (5): 315-398. http://dx.doi.org/10.1016/0370-1573(81)90190-3.
4. Brown, H. E., (1957): *Zinc oxide rediscovered*, New Jersey Zinc Company, New York.
5. Hahn, Y.-B., (2011): Zinc oxide nanostructures and their applications, *Kor. J. Chem. Eng.*, 28 (9): 1797-1813. http://dx.doi.org/10.1007/s11814-011-0213-3.
6. Klingshirn, C.; Fallert, J.; Zhou, H.; Sartor, J.; Thiele, C.; Maier-Flaig, F.; Schneider, D.; Kalt, H., (2010): 65 years of ZnO research - old and very recent results, *Phys. Status Solidi B*, 247 (6): 1424-1447. http://dx.doi.org/10.1002/pssb.200983195.
7. Moezzi, A.; McDonagh, A. M.; Cortie, M. B., (2012): Zinc oxide particles: Synthesis, properties and applications, *Chem. Eng. J.*, 185-186 (0): 1-22. http://dx.doi.org/10.1016/j.cej.2012.01.076.
8. Özgur, U.; Hofstetter, D.; Morkoç, H., (2010): ZnO devices and applications: A review of current status and future prospects, *Proc. IEEE*, 98 (7): 1255-1268. http://dx.doi.org/10.1109/JPROC.2010.2044550.
9. Schmidt-Mende, L.; MacManus-Driscoll, J. L., (2007): ZnO - nanostructures, defects, and devices, *Mater. Today*, 10 (5): 40-48. http://dx.doi.org/10.1016/S1369-7021(07)70078-0.
10. Klingshirn, C. R.; Meyer, B. K.; Waag, A.; Hoffmann, A.; Geurts, J., (2010): *Zinc Oxide: From Fundamental Properties Towards Novel Applications*, Springer, Heidelberg. http://dx.doi.org/10.1007/978-3-642-10577-7.
11. Joudrier, A.-L.; Levy, F.; Simon, N.; Bouttemy, M.; Levy, F.; Feuillet, G.; Etcheberry, A., (2010): Interfacial Electrochemistry of ZnO: An Influence of the Surface Polarity?, *ECS Trans.*, 25 (42): 21-27.
12. Dong, Y.; Fang, Z.-Q.; Look, D. C.; Cantwell, G.; Zhang, J.; Song, J. J.; Brillson, L. J., (2008): Zn- and O-face polarity effects at ZnO surfaces and metal interfaces, *Appl. Phys. Lett.*, 93 (7): 072111-3. http://dx.doi.org/10.1063/1.2974983.
13. Wöll, C., (2007): The chemistry and physics of zinc oxide surfaces, *Prog. Surf. Sci.*, 82 (2-3): 55-120. http://dx.doi.org/10.1016/j.progsurf.2006.12.002.
14. Tasker, P. W., (1979): The stability of ionic crystal surfaces, *J. Phys. C: Sol. State Phys.*, 12 (22): 4977. http://dx.doi.org/10.1088/0022-3719/12/22/036.
15. Kumar, R. K.; Husain, M.; Khan, Z. H., (2011): Optical studies on amorphous ZnO film, *Dig. J. Nanomater. Biostr.*, 6 (3): 1317-1323.
16. Hoon, J.-W.; Chan, K.-Y.; Tou, T.-Y., (2013): Zinc oxide films deposited by radio frequency plasma magnetron sputtering technique, *Ceram. Int.*, 39 (1): S269-S272. http://dx.doi.org/10.1016/j.ceramint.2012.10.075.
17. Swapna, R.; Santhosh Kumar, M. C., (2012): The role of substrate temperature on the properties of nanocrystalline Mo doped ZnO thin films by spray

pyrolysis, *Ceram. Int.*, 38 (5): 3875-3883. http://dx.doi.org/10.1016/j.ceramint.2012.01.039.
18. Yang, J.; Pei, Y.; Hu, R.; Fan, B.; Tong, C.; Kojima, T.; Wu, Z.; Jiang, H.; Wang, G., (2012): Morphology controlled synthesis of crystalline ZnO film by MOCVD: From hexagon to rhombus, *Crystengcomm*, 14 (24): 8345-8348. http://dx.doi.org/10.1039/c2ce26024g.
19. Mosca, M.; Macaluso, R.; Cali, C.; Butte, R.; Nicolay, S.; Feltin, E.; Martin, D.; Grandjean, N., (2013): Optical, structural, and morphological characterisation of epitaxial ZnO films grown by pulsed-laser deposition, *Thin Solid Films*, 539: 55-59. http://dx.doi.org/10.1016/j.tsf.2013.04.146.
20. Lewis, J. A., (2000): Colloidal Processing of Ceramics, *J. Am. Ceram. Soc.*, 83 (10): 2341-2359. http://dx.doi.org/10.1111/j.1151-2916.2000.tb01560.x.
21. Boccaccini, A. R.; Roether, J. A.; Thomas, B. J. C.; Shaffer, M. S. P.; Chavez, E.; Stoll, E.; Minay, E. J., (2006): The electrophoretic deposition of inorganic nanoscaled materials, *J. Ceram. Soc. Jpn.*, 114 (1325): 1-14. http://dx.doi.org/10.2109/jcersj.114.1.
22. Sarkar, P.; Nicholson, P. S., (1996): Electrophoretic deposition (EPD): Mechanisms, kinetics, and application to ceramics, *J. Am. Ceram. Soc.*, 79 (8): 1987-2002. http://dx.doi.org/10.1111/j.1151-2916.1996.tb08929.x.
23. Goodwin, J. W., (2004): *Colloids and Interfaces with Surfactants and Polymers - An Introduction.*, John Wiley & Sons, London. http://dx.doi.org/10.1002/0470093919.
24. Van Der Biest, O. O.; Vandeperre, L. J., (1999): Electrophoretic deposition of materials, *Annu. Rev. Mater. Sci.*, 29: 327-352. http://dx.doi.org/10.1146/annurev.matsci.29.1.327.
25. Shaw, D. J., (1992): *Introduction to colloid and surface chemistry*, Butterworth-Heinemann, Oxford.
26. Moreno, R., (2005): *Reología de suspensiones cerámicas*, CSIC, Madrid.
27. Osipov, V.; Sergeev, E., (1972): Crystallochemistry of clay minerals and their properties, *B. Eng. Geol. Environ.*, 5: 9-15. http://dx.doi.org/10.1007/BF02634646.
28. Swartzen-Allen, S. L.; Matijevic, E., (1975): Colloid and surface properties of clay suspensions: II. Electrophoresis and cation adsorption of montmorillonite, *J. Colloid Interface Sci.*, 50 (1): 143-153. http://dx.doi.org/10.1016/0021-9797(75)90261-1.
29. Swartzen-Allen, S. L.; Matijevic, E., (1976): Colloid and surface properties of clay suspensions. III. Stability of montmorillonite and kaolinite, *J. Colloid Interface Sci.*, 56 (1): 159-167. http://dx.doi.org/10.1016/0021-9797(76)90158-2.
30. Schroth, B. K.; Sposito, G., (1997): Surface charge properties of kaolinite, *Mater. Res. Soc. Symposium - Proceedings*, 432: 87-92. http://dx.doi.org/10.1557/PROC-432-87.
31. Sposito, G.; Skipper, N. T.; Sutton, R.; Park, S.-h.; Soper, A. K.; Greathouse, J. A., (1999): Surface geochemistry of the clay minerals *Proceedings of the National Academy of Sciences*, 96 (7): 3358-3364. http://dx.doi.org/10.1073/pnas.96.7.3358.
32. Kelso, J. F.; Ferrazzoli, T. A., (1989): Effect of Powder Surface Chemistry on the Stability of Concentrated Aqueous Dispersions of Alumina, *J. Am. Ceram. Soc.*, 72 (4): 625-627. http://dx.doi.org/10.1111/j.1151-2916.1989.tb06185.x.
33. Franks, G. V.; Gan, Y., (2007): Charging Behavior at the Alumina - Water Interface and Implications for Ceramic Processing, *J. Am. Ceram. Soc.*, 90 (11): 3373-3388. http://dx.doi.org/10.1111/j.1551-2916.2007.02013.x.
34. Diebold, U.; Li, S.-C.; Schmid, M., (2010): Oxide surface science, *Annu. Rev. Phys. Chem.*, 61: 129-148. http://dx.doi.org/10.1146/annurev.physchem.012809.103254.
35. Valtiner, M.; Torrelles, X.; Pareek, A.; Borodin, S.; Gies, H.; Grundmeier, G., (2010): In Situ Study of the Polar ZnO(0001)-Zn Surface in Alkaline Electrolytes, *J. Phys. Chem. C*, 114 (36): 15440-15447. http://dx.doi.org/10.1021/jp1047024.
36. Kresse, G.; Dulub, O.; Diebold, U., (2003): Competing stabilization mechanism for the polar ZnO(0001)-Zn surface, *Phys. Rev. B*, 68 (24): 245409. http://dx.doi.org/10.1103/PhysRevB.68.245409.
37. Losurdo, M.; Giangregorio, M. M.; Capezzuto, P.; Bruno, G.; Malandrino, G.; Blandino, M.; Fragalà, I. L., (2005): Reactivity of ZnO: Impact of polarity and nanostructure, *Superlattices Microstruct.*, 38 (4-6): 291-299. http://dx.doi.org/10.1016/j.spmi.2005.08.014.
38. Reed, J. S., (1986): *Introduction to the Principles of Ceramic Processing.*, John Wiley & Sons, New York.
39. Reichle, R. A.; McCurdy, K. G.; Hepler, L. G., (1975): Zinc Hydroxide: Solubility Product and Hydroxy-complex Stability Constants from 12.-75 °C, *Can. J. Chem.*, 53 (24): 3841-3845. http://dx.doi.org/10.1139/v75-556.
40. Blok, L.; Bruyn, P. L. D., (1970): The ionic double layer at the ZnO solution interface. I. The experimental point of zero charge, *J. Colloid Interface Sci.*, 32 (3): 518-526. http://dx.doi.org/10.1016/0021-9797(70)90142-6.
41. Logtenberg, E. H. P.; Stein, H. N., (1986): Surface charge and coagulation of aqueous ZnO dispersions, *J. Colloid Interface Sci.* , 109 (1): 190-200. http://dx.doi.org/10.1016/0021-9797(86)90294-8.
42. Parks, G. A., (1965): The isoelectric points of solid oxides, solid hydroxides, and aqueous hydroxo complex systems, *Chem. Rev.*, 65 (2): 177-198. http://dx.doi.org/10.1021/cr60234a002.
43. Degen, A.; Kosec, M., (2000): Effect of pH and impurities on the surface charge of zinc oxide in aqueous solution, *J. Eur. Ceram. Soc.*, 20 (6): 667-673. http://dx.doi.org/10.1016/S0955-2219(99)00203-4.
44. Cao, G., (2004): *Nanostructures and Nanomaterials: Synthesis, Properties, and Applications*, Imperial College Press, London. http://dx.doi.org/10.1142/9781860945960.
45. Tang, E.; Cheng, G.; Ma, X.; Pang, X.; Zhao, Q., (2006): Surface modification of zinc oxide nanoparticle by PMAA and its dispersion in aqueous system, *Appl. Surf. Sci.*, 252 (14): 5227-5232. http://dx.doi.org/10.1016/j.apsusc.2005.08.004.
46. Liufu, S.; Xiao, H.; Li, Y., (2004): Investigation of PEG adsorption on the surface of zinc oxide nanoparticles, *Powder Technol.*, 145 (1): 20-24. http://dx.doi.org/10.1016/j.powtec.2004.05.007.
47. Tang, F., T. Uchikoshi, Y. Sakka, (2002): Electrophoretic Deposition Behavior of Aqueous Nanosized Zinc Oxide Suspensions, *J. Am. Ceram. Soc.*, 85 (9): 2161-2165. http://dx.doi.org/10.1111/j.1151-2916.2002.tb00428.x.
48. Tang, F.; Sakka, Y.; Uchikoshi, T., (2003): Electrophoretic deposition of aqueous nano-sized zinc oxide suspensions on a zinc electrode, *Mater. Res. Bull.*, 38 (2): 207-212. http://dx.doi.org/10.1016/S0025-5408(02)01029-2.
49. Verde, M.; Caballero, A. C.; Iglesias, Y.; Villegas, M.; Ferrari, B., (2010): Electrophoretic deposition of flake-shaped ZnO nanoparticles, *J. Electrochem. Soc.*, 157 (1): H55-H59. http://dx.doi.org/10.1149/1.3247343.
50. Verde, M.; Peiteado, M.; Caballero, A. C.; Villegas, M.; Ferrari, B., (2012): Electrophoretic Deposition of Transparent ZnO Thin Films from Highly Stabilized Colloidal Suspensions, *J. Colloid Interface Sci.*, 373 (1): 27-33. http://dx.doi.org/10.1016/j.jcis.2011.09.039.
51. Crea, F.; Crea, P.; De Robertis, A.; Sammartano, S., (2007): Thermodynamic study for the protonation of branched poly(ethylenimine) in NaCl(aq) and its dependence on ionic strength, *J. Chem. Eng. Data*, 52 (1): 279-285. http://dx.doi.org/10.1021/je060388z.
52. Dange, C.; Phan, T. N. T.; André, V.; Rieger, J.; Persello, J.; Foissy, A., (2007): Adsorption mechanism and dispersion efficiency of three anionic additives [poly(acrylic acid), poly(styrene sulfonate) and HEDP] on zinc oxide, *J. Colloid Interface Sci.*, 315 (1): 107-115. http://dx.doi.org/10.1016/j.jcis.2007.03.068.
53. Bahnemann, D. W.; Kormann, C.; Hoffmann, M. R., (1987): Preparation and characterization of quantum size zinc oxide: a detailed spectroscopic study, *J. Phys. Chem.*, 91 (14): 3789-3798. http://dx.doi.org/10.1021/j100298a015.
54. Logtenberg, E. H. P.; Stein, H. N., (1986): Zeta potential and coagulation of ZnO in alcohols, *Colloid Surf.* , 17 (3): 305-312. http://dx.doi.org/10.1016/0166-6622(86)80254-2.
55. Ghashghaie, S.; Marzbanrad, E.; Raissi Dehkordi, B., (2011): Low-frequency electrophoretic deposition of ZnO nanoparticles: Effect of organic medium on deposition pattern, *J. Am. Ceram. Soc.*, 94 (10): 3431-3436. http://dx.doi.org/10.1111/j.1551-2916.2011.04527.x.
56. Meulenkamp, E. A., (1998): Synthesis and Growth of ZnO Nanoparticles, *J. Phys. Chem. B.*, 102 (29): 5566-5572. http://dx.doi.org/10.1021/jp980730h.
57. Sakohara, S.; Ishida, M.; Anderson, M. A., (1998): Visible Luminescence and Surface Properties of Nanosized ZnO Colloids Prepared by Hydrolyzing Zinc Acetate, *J. Phys. Chem. B*, 102 (50): 10169-10175. http://dx.doi.org/10.1021/jp982594m.
58. Yang, R. D.; Tripathy, S.; Li, Y.; Sue, H.-J., (2005): Photoluminescence and micro-Raman scattering in ZnO nanoparticles: The influence of acetate adsorption, *Chem. Phys. Lett.*, 411 (1–3): 150-154. http://dx.doi.org/10.1016/j.cplett.2005.05.125.
59. Marczak, R.; Segets, D.; Voigt, M.; Peukert, W., (2010): Optimum between purification and colloidal stability of ZnO nanoparticles, *Adv. Powder Technol.*, 21 (1): 41-49. http://dx.doi.org/10.1016/j.apt.2009.10.005.
60. Segets, D.; Marczak, R.; Schäfer, S.; Paula, C.; Gnichwitz, J.-F.; Hirsch, A.; Peukert, W., (2011): Experimental and Theoretical Studies of the Colloidal Stability of Nanoparticles−A General Interpretation Based on Stability Maps, *ACS Nano*, 5 (6): 4658-4669. http://dx.doi.org/10.1021/nn200465b.
61. Wang, Y. C.; Leu, I. C.; Hon, M. H., (2002): Effect of colloid characteristics on the fabrication of ZnO nanowire arrays by electrophoretic deposition., *J. Mater. Chem.*, 12 (8): 2439-2444. http://dx.doi.org/10.1039/b111189m.
62. Sun, D.; Wong, M.; Sun, L.; Li, Y.; Miyatake, N.; Sue, H. J., (2007): Purification and stabilization of colloidal ZnO nanoparticles in methanol, *J. Sol-Gel Sci. Technol.*, 43 (2): 237-243. http://dx.doi.org/10.1007/s10971-007-1569-z.
63. Ma, S. R.; Shi, L. Y.; Feng, X.; Yu, W. J.; Lu, B., (2008): Graft modification of ZnO nanoparticles with silane coupling agent KH570 in mixed solvent, *J. Shanghai Uni.*, 12 (3): 278-282. http://dx.doi.org/10.1007/s11741-008-0316-1.
64. Hong; L. L. Chen; J. H. Li; H. Z. Li; Y. Zheng; J. Ding, (2007): Preparation and application of polystyrene-grafted ZnO nanoparticles, *Polym. Adv. Technol.*, 18 (11): 901-909.
65. Wu, K.; Zhitomirsky, I., (2010): Electrophoretic Deposition of Ceramic Nanoparticles, *Int. J. Appl. Ceram. Technol.*, 920-927.
66. Hamaker, H. C., (1940): Formation of a deposit by electrophoresis, *Trans. Faraday Soc.*, 35 279-287. http://dx.doi.org/10.1039/tf9403500279.
67. Wong, E. M.; Searson, P. C., (1999): Kinetics of electrophoretic deposition of zinc oxide quantum particle thin films, *Chem. Mater.*, 11 (8): 1959-1961. http://dx.doi.org/10.1021/cm990264o.
68. Wang, Y., I. C. Leu, M.H. Hon, (2004): Kinetics of Electrophoretic Deposition for Nanocrystalline Zinc Oxide Coatings, *J. Am. Ceram. Soc.*, 87 (1): 84-88. http://dx.doi.org/10.1111/j.1551-2916.2004.00084.x.
69. Lommens, P.; Van Thourhout, D.; Smet, P. F.; Poelman, D.; Hens, Z., (2008): Electrophoretic deposition of ZnO nanoparticles, from micropatterns to substrate coverage, *Nanotechnology*, 19 (24): 245-301. http://dx.doi.org/10.1088/0957-4484/19/24/245301.

70. Balaji, J.; Boominathasellarajan, S.; Sasikala, N. T.; Raghupathy, B. P. C., (2011): Electrophoretic deposition of ZNO nanorods and nanoparticles, *Int. J. Nanosci.*, 10 (4-5): 787-792. http://dx.doi.org/10.1142/S0219581X11008903.
71. Miao, L.; Cai, S.; Xiao, Z., (2010): Preparation and characterization of nanostructured ZnO thin film by electrophoretic deposition from ZnO colloidal suspensions, *J. Alloy. Compd.*, 490 (1-2): 422-426. http://dx.doi.org/10.1016/j.jallcom.2009.10.021.
72. Wang, Y. C.; Leu, I. C.; Hon, M. H., (2002): Preparation and characterization of nanosized ZnO arrays by electrophoretic deposition, *J. Cryst. Growth*, 237-239 (1-4 I): 564-568.
73. Wang, Y. C.; Leu, I. C.; Hon, M. H., (2004): Dielectric property and structure of anodic alumina template and their effects on the electrophoretic deposition characteristics of ZnO nanowire arrays, *J. Appl. Phys.*, 95 (3): 1444-1449. http://dx.doi.org/10.1063/1.1637710.
74. Wang, Y. -C.; Leu, I. -C.; Hon, M. -H., (2002): Preparation of nanosized ZnO arrays by electrophoretic deposition, *Electrochem. Sol. State Lett.*, 5 (4): C53-C55. http://dx.doi.org/10.1149/1.1454547.
75. Wang, Y. -C.; Leu, I. -C.; Hon, M. -H., (2004): Size control of ZnO nanofibril within template by electrophoretic deposition, *Electrochem. Sol. State Lett.*, 7 (10).
76. Chung, Y. -W.; Leu, I. -C.; Lee, J. -H.; Hon, M. -H., (2009): Electrophoretic deposition kinetics of ZnO nanoparticles into an opal template and fabrication of well-ordered macroporous structure, *J Electrochem. Soc*, 156 (6): E91-E95. http://dx.doi.org/10.1149/1.3098473.
77. Chung, Y. -W.; Leu, I. -C.; Lee, J. -H.; Hon, M. -H., (2009): Filling behavior of ZnO nanoparticles into opal template via electrophoretic deposition and the fabrication of inverse opal, *Electrochim. Acta*, 54 (13): 3677-3682. http://dx.doi.org/10.1016/j.electacta.2009.01.013.
78. Lee, J. -H.; Leu, I. -C.; Chung, Y. -W.; Hon, M. -H., (2006): Fabrication of ordered ZnO hierarchical structures controlled via surface charge in the electrophoretic deposition process, *Nanotechnology*, 17 (17): 4445-4450. http://dx.doi.org/10.1088/0957-4484/17/17/027.
79. Verde, M.; Peiteado, M.; Villegas, M.; Ferrari, B.; Caballero, A. C., (2013): Soft solution processing of ZnO nanoarrays by combining electrophoretic deposition and hydrothermal growth, *Mater. Chem. Phys.*, 140 (1): 75-80. http://dx.doi.org/10.1016/j.matchemphys.2013.02.067.
80. Haas-Santo, K.; Görke, O.; Pfeifer, P.; Schubert, K., (2002): Catalyst coatings for microstructure reactors, *Chimia*, 56 (11): 605-610. http://dx.doi.org/10.2533/000942902777679993.
81. Nedyalkova, R.; Casanovas, A.; Llorca, J.; Montané, D., (2009): Electrophoretic deposition of Co-Me/ZnO (Me = Mn,Fe) ethanol steam reforming catalysts on stainless steel plates, *Int. J. Hydrog. Energy*, 34 (6): 2591-2599. http://dx.doi.org/10.1016/j.ijhydene.2009.01.050.
82. Huang, Y.; Sarkar, D. K.; Chen, X. G., (2014): Fabrication of superhydrophobic aluminum surfaces by chemical etching and electrophoretic deposition processes for corrosion application, *Proc. Mater. Sci. Technol. Conf. 2013, Montreal, QC.*, 4: 2279-2284.
83. Barsan, N.; Koziej, D.; Weimar, U., (2007): Metal oxide-based gas sensor research: How to?, *Sens. Act. B: Chem.*, 121 (1): 18-35. http://dx.doi.org/10.1016/j.snb.2006.09.047.
84. Korotcenkov, G., (2005): Gas response control through structural and chemical modification of metal oxide films: state of the art and approaches, *Sens. Act. B: Chem.*, 107 (1): 209-232. http://dx.doi.org/10.1016/j.snb.2004.10.006.
85. Hossein-Babaei, F.; Taghibakhsh, F., (2000): Electrophoretically deposited zinc oxide thick film gas sensor, *Electron. Lett.*, 36 (21): 1815-1816. http://dx.doi.org/10.1049/el:20001258.
86. Dougami, N.; Takada, T., (2003): Modification of metal oxide semiconductor gas sensor by electrophoretic deposition, *Sens. Act. B*, 93 (1-3): 316-320. http://dx.doi.org/10.1016/S0925-4005(03)00219-3.
87. Rout, C. S.; Hari Krishna, S.; Vivekchand, S. R. C.; Govindaraj, A.; Rao, C. N. R., (2006): Hydrogen and ethanol sensors based on ZnO nanorods, nanowires and nanotubes, *Chem. Phys. Lett.*, 418 (4-6): 586-590. http://dx.doi.org/10.1016/j.cplett.2005.11.040.
88. Rout, C. S.; Raju, A. R.; Govindaraj, A.; Rao, C. N. R., (2007): Ethanol and hydrogen sensors based on ZnO nanoparticles and nanowires, *J. Nanosci. Nanotechnol.*, 7 (6): 1923-1929. http://dx.doi.org/10.1166/jnn.2007.742.
89. Han, N.; Deng, P.; Chen, J.; Chai, L.; Gao, H.; Chen, Y., (2010): Electrophoretic deposition of metal oxide films aimed for gas sensors application: The role of anodic aluminum oxide (AAO)/Al composite structure, *Sens. Act. B: Chem.*, 144 (1): 267-273. http://dx.doi.org/10.1016/j.snb.2009.10.068.
90. Wong, E. M.; Searson, P. C., (1999): ZnO quantum particle thin films fabricated by electrophoretic deposition, *Appl. Phys. Lett.*, 74 (20): 2939-2941. http://dx.doi.org/10.1063/1.123972.
91. Djurisic, A. B.; Leung, Y. H., (2006): Optical Properties of ZnO Nanostructures, *Small*, 2 (8-9): 944-961. http://dx.doi.org/10.1002/smll.200600134.
92. Klingshirn, C. F., (2007): ZnO: Material, physics and applications, *ChemPhysChem*, 8 (6): 782-803. http://dx.doi.org/10.1002/cphc.200700002.
93. Norton, D. P.; Heo, Y. W.; Ivill, M. P.; Ip, K.; Pearton, S. J.; Chisholm, M. F.; Steiner, T., (2004): ZnO: Growth, doping & processing, *Mater. Today*, 7 (6): 34-40. http://dx.doi.org/10.1016/S1369-7021(04)00287-1.
94. Jeon, B.-S.; Yoo, J. S.; Lee, J. D., (1996): Electrophoretic Deposition of ZnO:Zn Phosphor for Field Emission Display Applications, *J. Electrochem. Soc.*, 143 (12): 3923-3927. http://dx.doi.org/10.1149/1.1837317.
95. Ma, L. A.; Guo, T. L., (2013): Morphology control and improved field emission properties of ZnO tetrapod films deposited by electrophoretic deposition, *Ceram. Int.*, 39 (6): 6923-6929. http://dx.doi.org/10.1016/j.ceramint.2013.02.027.
96. Wang, Z.; Zhang, H.; Wang, Z.; Zhang, L.; Yuan, J.; Yan, S.; Wang, C., (2003): Structure and strong ultraviolet emission characteristics of amorphous ZnO films grown by electrophoretic deposition, *J. Mater. Res.*, 18 (1): 151-155. http://dx.doi.org/10.1557/JMR.2003.0021.
97. Zhang, H.; Cui, Y.; Men, Y.; Liu, X., (2006): Strong ultraviolet emission from zinc oxide thin films prepared by electrophoretic deposition, *J. Lumin.*, 121 (2): 601-605. http://dx.doi.org/10.1016/j.jlumin.2005.12.056.
98. Yadav, H. K.; Gupta, V., (2012): A comparative study of ultraviolet photoconductivity relaxation in zinc oxide (ZnO) thin films deposited by different techniques, *J. Appl. Phys.*, 111 (10). http://dx.doi.org/10.1063/1.4714715.
99. Grätzel, M., (2001): Photoelectrochemical cells, *Nature*, 414 (6861): 338-344. http://dx.doi.org/10.1038/35104607.
100. Grätzel, M., (2003): Dye-sensitized solar cells, *J. Photochem. Photobio. C: Photochem. Rev.*, 4 (2): 145-153. http://dx.doi.org/10.1016/S1389-5567(03)00026-1.
101. Yamaguchi, T.; Tobe, N.; Matsumoto, D.; Nagai, T.; Arakawa, H., (2010): Highly efficient plastic-substrate dye-sensitized solar cells with validated conversion efficiency of 7.6%, *Sol. Energy Mater. Sol. Cells*, 94 (5): 812-816. http://dx.doi.org/10.1016/j.solmat.2009.12.029.
102. Chen, W.; Zhang, H.; Hsing, I. M.; Yang, S., (2009): A new photoanode architecture of dye sensitized solar cell based on ZnO nanotetrapods with no need for calcination, *Electrochem. Commun.*, 11 (5): 1057-1060. http://dx.doi.org/10.1016/j.elecom.2009.03.013.
103. Chen, Z.; Tang, Y.; Zhang, L.; Luo, L., (2006): Electrodeposited nanoporous ZnO films exhibiting enhanced performance in dye-sensitized solar cells, *Electrochim. Acta*, 51 (26): 5870-5875. http://dx.doi.org/10.1016/j.electacta.2006.03.026.
104. Hosono, E.; Mitsui, Y.; Zhou, H., (2008): Metal-free organic dye sensitized solar cell based on perpendicular zinc oxide nanosheet thick films with high conversion efficiency, *Dalton Trans.*, (40): 5439-5441. http://dx.doi.org/10.1039/b800907d.
105. Saito, M.; Fujihara, S., (2008): Large photocurrent generation in dye-sensitized ZnO solar cells, *Energy Env. Sci.*, 1 (2): 280-283. http://dx.doi.org/10.1039/b806096g.
106. Zhang, Q.; Chou, T. P.; Russo, B.; Jenekhe, S. A.; Cao, G., (2008): Aggregation of ZnO nanocrystallites for high conversion efficiency in dye-sensitized solar cells, *Angew. Chem.-Int. Edit.*, 47 (13): 2402-2406. http://dx.doi.org/10.1002/anie.200704919.
107. Zhang, W.; Zhu, R.; Liu, X.; Liu, B.; Ramakrishna, S., (2009): Facile construction of nanofibrous ZnO photoelectrode for dye-sensitized solar cell applications, *Appl. Phys. Lett.*, 95 (4). http://dx.doi.org/10.1063/1.3193661.
108. Jiang, C. Y.; Sun, X. W.; Tan, K. W.; Lo, G. Q.; Kyaw, A. K. K.; Kwong, D. L., (2008): High-bendability flexible dye-sensitized solar cell with a nanoparticle-modified ZnO-nanowire electrode, *Appl. Phys. Lett.*, 92 (14). http://dx.doi.org/10.1063/1.2905271.
109. Yoshida, T.; Zhang, J.; Komatsu, D.; Sawatani, S.; Minoura, H.; Pauporté, T.; Lincot, D.; Oekermann, T.; Schlettwein, D.; Tada, H.; Wöhrle, D.; Funabiki, K.; Matsui, M.; Miura, H.; Yanagi, H., (2009): Electrodeposition of inorganic/organic hybrid thin films, *Adv. Funct. Mater.*, 19 (1): 17-43. http://dx.doi.org/10.1002/adfm.200700188.
110. Yin, X.; Liu, X.; Wang, L.; Liu, B., (2010): Electrophoretic deposition of ZnO photoanode for plastic dye-sensitized solar cells, *Electrochem. Commun.*, 12 (9): 1241-1244. http://dx.doi.org/10.1016/j.elecom.2010.06.029.
111. Chen, H.-W.; Lin, C.-Y.; Lai, Y.-H.; Chen, J.-G.; Wang, C.-C.; Hu, C.-W.; Hsu, C.-Y.; Vittal, R.; Ho, K.-C., (2011): Electrophoretic deposition of ZnO film and its compression for a plastic based flexible dye-sensitized solar cell, *J. Power Sources*, 196 (10): 4859-4864. http://dx.doi.org/10.1016/j.jpowsour.2011.01.057.
112. Hara, Y.; Brownson, J. R. S.; Anderson, M. A., (2012): Fabrication of Thin-Films Composed of ZnO Nanorods Using Electrophoretic Deposition, *Int. J. Appl. Ceram. Technol.*, 9 (1): 115-123. http://dx.doi.org/10.1111/j.1744-7402.2011.02638.x.
113. Hara, Y.; Tejedor-Tejedor, M. I.; Brzozowski, L. J.; Lara, K.; Lubin, D.; Severseike, D. J.; Anderson, M. A., (2011): Adsorption isotherms in defining performance of dye-sensitized solar cells with photoelectrodes of TiO2 and ZnO, *J. Electrochem. Soc.*, 158 (11): B1417-B1422. http://dx.doi.org/10.1149/2.070111jes.
114. Hara, Y.; Tejedor-Tejedor, M. I.; Lara, K.; Lubin, D.; Brzozowski, L. J.; Severseike, D. J.; Anderson, M. A., (2011): Importance of adsorption isotherms in defining performance of dye-sensitized solar cells fabricated from photoelectrodes composed of ZnO nanopowders and nanorods, *Electrochim. Acta*, 56 (24): 8873-8879. http://dx.doi.org/10.1016/j.electacta.2011.07.103.
115. Yan, L. T.; Wu, F. L.; Peng, L.; Zhang, L. J.; Li, P. J.; Dou, S. Y.; Li, T. X., (2012): Photoanode of dye-sensitized solar cells based on a ZnO/TiO 2 composite film, *Int. J. Photoenergy*, 2012 .
116. Sima, M.; Vasile, E.; Sima, A., (2013): Photoanode for dye-sensitized solar cell based on electrophoretically deposited ZnO layer, *Dig. J. Nanomat. Biostr.*, 8 (2): 757-763.

Recibido: 20/03/2014
Recibida versión corregida: 16/04/2014
Aceptado: 23/04/2014